Biochimica et Biophysica Acta 1853 (2015) 1606–1614

Contents lists available at ScienceDirect

Biochimica et Biophysica Acta

journal homepage: www.elsevier.com/locate/bbamcr

Rotenone inhibits primary murine myotube formation via Raf-1 and ROCK2

Sander Grefte, Jori A.L. Wagenaars, Renate Jansen, Peter H.G.M. Willems, Werner J.H. Koopman *

Department of Biochemistry, Radboud Institute for Molecular Life Sciences, Radboud University Medical Center, Nijmegen, The Netherlands

ARTICLE INFO

Article history:
Received 20 November 2014
Received in revised form 4 March 2015
Accepted 19 March 2015
Available online 28 March 2015

Keywords:
Fusion index
GW5074
U0126
Rotenone
Piericidin A
Rho-GTPase

ABSTRACT

Rotenone (ROT) is a widely used inhibitor of complex I (CI), the first complex of the mitochondrial oxidative phosphorylation (OXPHOS) system. However, particularly at high concentrations ROT was also described to display off-target effects. Here we studied how ROT affected *in vitro* primary murine myotube formation. We demonstrate that myotube formation is specifically inhibited by ROT (10–100 nM), but not by piericidin A (PA; 100 nM), another CI inhibitor. At 100 nM, both ROT and PA fully blocked myoblast oxygen consumption. Knock-down of Rho-associated, coiled-coil containing protein kinase 2 (ROCK2) and, to a lesser extent ROCK1, prevented the ROT-induced inhibition of myotube formation. Moreover, the latter was reversed by inhibiting Raf-1 activity. In contrast, ROT-induced inhibition of myotube formation was not prevented by knock-down of RhoA. Taken together, our results support a model in which ROT reduces primary myotube formation independent of its inhibitory effect on CI-driven mitochondrial ATP production, but via a mechanism primarily involving the Raf-1/ROCK2 pathway.

1. Introduction

Rotenone (ROT) is an agricultural pesticide, insecticide and pisciside. ROT is well-known to exerts its effect by inhibiting complex I (CI or NADH:ubiquinone oxidoreductase; EC 1.6.5.3) of the mitochondrial oxidative phosphorylation (OXPHOS) system, which is among the prime generators of cellular ATP to sustain cell function and survival [1,2]. The latter system consists of five multiprotein complexes (CI–CV), which consume NADH, succinate and molecular oxygen to generate ATP by chemiosmotic coupling [3]. In this sense, ROT treatment is widely used to study the consequences of CI inhibition and ensuing OXPHOS dysfunction [4].

Skeletal muscle is a high-energy demanding tissue and therefore an attractive model to study CI- or OXPHOS dysfunction. Within skeletal muscle, satellite cells play a crucial role [5,6]. *In vitro* differentiation of satellite cells (aka myoblasts) into myotubes can be triggered by transferring the former cells from a proliferation to a differentiation medium [7–9]. This differentiation process shares many features with the *in vivo* myogenic differentiation program and consists of a proliferation, differentiation and fusion phase [10–12]. Evidence was provided that myotube formation requires mitochondrial activity [13–19] and is paralleled by mitochondrial biogenesis, increased expression of OXPHOS complexes and higher cellular oxygen consumption [20,21]. Moreover, ROT treatment inhibited *in vitro* myotube formation [22,23], suggesting that active CI is required for proper myoblast differentiation. However, ROT can also induce other effects than CI inhibition, which include microtubule depolarization and altering the activity of RhoA, Cdc42 and Rac1, which are members of the Rho family of small GTPases [24,25]. This leaves open the possibility that a CI-independent mechanism is involved in ROT-induced inhibition of myotube formation [22,23]. In fact, RhoA activity is required during early myoblast differentiation [26], while Rac1 and Cdc42 negatively regulate this process [27–29]. Conversely, at the final stage of differentiation (i.e. myotube formation), the activity of RhoA and its effector Rho-associated, coiled-coil containing protein kinase (ROCK) must be decreased [30–32], while Rac1 and Cdc42 activity is essential [33]. As ROT increases RhoA activity in neurons and thereby, via ROCK activity, prevented *in vitro* axon formation [25], we hypothesize that the ROT-induced inhibition of myotube formation could be mediated by the RhoA/ROCK pathway.

Here we demonstrate that ROT, but not the CI inhibitor piericidin A (PA), inhibits primary myotube formation when used at the lowest concentration that fully blocks cellular oxygen consumption. Subsequent RNA interference and inhibitor studies revealed that this inhibition depends on Raf-1 and ROCK2 (and to a lesser extend ROCK1), but not RhoA.

Abbreviations: CI, complex I; ETC, electron transport chain; HEt, hydroethidium; Oas1, 2,5-oligoadenylate synthetase; OXPHOS, oxidative phosphorylation; PA, piericidin A; ROS, reactive oxygen species; ROT, rotenone

* Corresponding author at: Department of Biochemistry (286), Radboud Institute for Molecular Life Sciences (RIMLS), Radboud University Medical Center (RUMC), P.O. Box 9101, NL-6500 HB Nijmegen, The Netherlands. Tel.: +31 24 3614589; fax: +31 24 3616413.

E-mail address: Werner.Koopman@radboudumc.nl (W.J.H. Koopman).

http://dx.doi.org/10.1016/j.bbamcr.2015.03.010
0167-4889/

2. Materials and methods

2.1. Animals and housing conditions

Wild-type (WT) mice were bred with a mixed 129/sv × C57BL/6 background. All animals received a standard rodent diet *ad libitum* and were maintained at 21.0 °C and 60% humidity, and with a light/dark (12 h/12 h) cycle. All breeding and experiments were approved by the Animal Experimentation Committee at the Radboud University Medical Center, in accordance with Dutch laws and regulations regarding animal experimentation.

2.2. Myofiber and primary myoblast isolation

Female WT mice (8–12 weeks) were sacrificed by decapitation and *extensor digitorum longus* (EDL) muscles were dissected. Individual myofibers were isolated as described in detail elsewhere [34]. Briefly, EDL muscles were digested in 0.2% (w/v) Collagenase type I (Sigma Chemical CO, St Louis, MO, USA) in high-glucose (25 mM) Dulbecco's Modified Eagle's medium (DMEM-HG; Invitrogen HQ, San Diego, CA, USA) + 1% penicillin/streptomycin (p/s, PAA Laboratories, Cölbe, Germany) for 1.5 h. Using a heat-polished wide-mouthed glass pipette, myofibers were liberated. Individual myofibers were transferred to a new Petri dish containing DMEM-HG + 1% p/s with a heat-polished small-mouthed glass pipette. Each Petri dish containing one-hundred fifty myofibers were washed by replacing the medium with fresh DMEM-HG + 1% p/s. Washed myofibers were plated onto 6-well plates coated with Matrigel (Matrigel™ Basement Membrane Matrix, BD Bioscience, Bedford, MA, USA) and containing 6 ml culture medium (CM; DMEM-HG supplemented with 30% (v/v) fetal bovine serum (FBS, PAA Laboratories), 10% (v/v) horse serum (HS, PAA Laboratories), 1% (v/v) chick embryo extract (CEE, MP Biomedicals Europe, Illkirch Cedex, France), 10 ng/ml basic fibroblast growth factor (bFGF; Invitrogen), and 1% (v/v) p/s (PAA Laboratories)). Next, the cells were cultured for three days at 37 °C (95% air, 5% CO_2), during which satellite cells grew out of the myofibers. After removal of the myofibers, satellite cells were trypsinized and pre-plated for 10 min in uncoated 6-well plate. Non-adherent cells were transferred to a fresh Matrigel-coated 6-well plate, cultured for 1 week in CM, and then used for experiments.

2.3. Primary myoblast cell culture

Coverslips (∅14 mm) were coated first with 20 μg/ml fibronectin (Roche Diagnostics GmbH, Mannheim, Germany) and subsequently with 10 μl Matrigel (1 mg/ml) to create a "Matrigel-spot" for the cells. A total of 5,000 primary myoblasts were seeded onto the Matrigel-spot in 10 μl CM and incubated for 10 min at 37 °C (95% air, 5% CO_2) for adherence. Next, 0.5 ml CM was added and cells were cultured at 37 °C (95% air, 5% CO_2) for 4 h. Then, differentiation and fusion of myoblasts was induced by replacing the CM by differentiation medium (DM; DMEM-HG supplemented with 2% (v/v) HS (PAA Laboratories) and 1% (v/v) p/s) and culturing the cells for an additional 3 days. Depending on the experiment, differentiation of primary myoblasts was carried out in the presence of vehicle (0.1% (v/v) EtOH), 0–100 nM ROT (Sigma), or 0–100 nM PA (Enzo Life Sciences, Farmingdale, NY, USA). Primary myoblasts were also differentiated in the presence of 100 nM ROT with or without 0–10 μM of GW5074 or U0126 (both Sigma).

2.4. C2C12 cell culture

C2C12 myoblasts were cultured in DMEM-HG (Invitrogen) supplemented with 10% (v/v) FBS and 1% (v/v) p/s and in the presence of either vehicle (0.1% (v/v) EtOH), 100 nM ROT (Sigma) or 100 nM PA (Sigma). After 3 days cells were used for high-resolution respirometry.

2.5. High-resolution respirometry of C2C12 myoblasts

The DMEM-HG culture medium was collected, and the C2C12 myoblasts were trypsinized, washed and resuspended to approximately one million cells per 2 ml in the collected culture medium and used to measure cellular oxygen consumption. Oxygen consumption was measured at 37 °C using polarographic oxygen sensors in a two-chamber Oxygraph (Oroboros Instruments, Innsbruck, Austria) using an established protocol [35]. Briefly, untreated cells were first allowed to respire at basal level for 10 min and then inhibited acutely by a stepwise addition of increasing concentrations (0–1000 nM) of either ROT (Sigma) or PA (Enzo Life Sciences) until respiration was maximally blocked. Basal (routine) respiration was set at 100% to which all other data points were related. A logistic model (nonlinear regression; Y = Bottom + (Top − Bottom) / (1 + 10^((LogIC50 − X) * HillSlope))) was created to determine the IC_{50} of each inhibitor. C2C12 myoblasts treated with vehicle (0.1% (v/v) EtOH), ROT, or PA for 3 days were also first allowed to respire at basal level for 10 min after which ROT and antimycin A were added to determine non-mitochondrial oxygen consumption rates.

2.6. Hydroethidium oxidation and quantification in primary myotubes

To measure the level of hydroethidium (HEt) oxidizing reactive oxygen species (ROS), myoblasts were first differentiated in the presence of 100 nM ROT or PA for 3 days. Then cells were loaded with 10 μM HEt (Molecular Probes, Eugene, OR, USA) in the ROT- and PA-containing DM for exactly 4.5 min. Finally, the cells were washed and transferred to a HEPES–Tris medium (132 mM NaCl, 4.2 mM KCl, 1 mM $CaCl_2$, 1 mM $MgCl_2$, 5.5 mM D-glucose and 10 mM HEPES, pH 7.4). The coverslips were mounted in an incubation chamber and placed on the stage of a inverted microscope (Axiovert 200 M, Carl Zeiss, Germany). Cells were excited at 490 nm for 100 ms using a monochromator (Polychrome IV, TILL Photonics, Gräfelfing, Germany) and fluorescence emission was directed by a 525DRLP dichroic mirror (Omega Optical Inc, Brattleboro, VT, USA) and through a 565ALP emission filter (Omega Optical Inc.). Cells were visualized using the Zeiss 40×/1.3 NA Plan NeoFluar objective and a CoolSNAP HQ monochrome CCD-camera (Roper Scientific, Vianen, The Netherlands) and the Metafluor 6.0 software (Universal Imaging Corporation, Downingtown, PA, USA). Quantitative analyses were performed with the Metamorph 6.0 software (Universal Imaging Corporation). For analysis, the mean fluorescent intensity in an intracellular region in at least 10 different microscopic fields was determined and corrected for background using an extracellular region of the same size. The average values were related to the average value of WT myotubes treated with vehicle (0.1% (v/v) EtOH), which was set at 100%.

2.7. Transfection of primary myoblasts with small interfering RNA molecules

Primary myoblasts were transfected with the Dharmacon siGENOME SMARTpool siRNAs (Thermo Fisher Scientific, Pittsburgh, PA); RhoA (M-042634-01), ROCK1 (M-046504-01), ROCK2 (M-040429-01), or Non-targeting (control pool, D-001206-13-05). For every siRNA, 900,000 myoblasts were transfected with 900 pmol siRNA using the Neon Transfection™ system (Invitrogen, Carlsbad, CA, USA) with a single pulse of 1350 V and a pulse width of 30, according to manufacturer's protocol. After transfection, myoblasts were seeded either into a Matrigel-coated 24-well plate (200,000 cells; 4 wells/transfection) or onto "Matrigel-spots" (10,000 cells; 2 spots/transfection) on a coverslip (∅14 mm) and cultured in CM for 1 day. Twenty-four hours after the transfection, the cells in the 24-well plate were differentiated in DM for 3 days (HS with a different lot was used: B02311-7049), and the myoblasts on the "Matrigel-spot" were differentiated in DM in the presence of either vehicle (0.1% EtOH) or 100 nM ROT for 3 days. To assess the

knock-down of RhoA, ROCK1, and ROCK2, proteins were isolated from untreated myoblasts (D0) and myotubes (D3).

2.8. Western blotting

Myoblasts were washed with PBS and lysed by scratching the cells from the wells using 50 μl RIPA buffer containing 50 mM Tris–HCl, 50 mM NaCl, 1% (v/v) Triton X-100, 5 mM Na-EDTA, 10 mM $Na_4P_2O_7$, 50 mM NaF, 1× protease inhibitor cocktail (Complete, Roche), 1 mg/ml DNAse, and 10 mM PMSF. Proteins (150 μg protein per lane) were separated using SDS-PAGE with a 12% gel for RhoA and a 6% gel for ROCK1 and ROCK2, and subsequently transferred to a PVDF membrane (Millipore, Amsterdam, The Netherlands). Then blots were blocked in Odyssey blocking buffer (Li-Cor, Lincoln, USA) and PBS/Tween-20 (1:1) and incubated with mouse anti-beta-actin (1:100,000; Sigma), mouse anti-RhoA (1:1000; Cytoskeleton, Denver, CO, USA), rabbit anti-ROCK1 (1:2000; Millipore), and rabbit anti-ROCK2 (1:10,000; Abcam, Cambridge, MA, USA) at 4 °C overnight. Bound anti-beta-actin and anti-RhoA were visualized using IRdye680-labeled goat-anti-mouse IgG (H + L; Li-Cor). Bound anti-ROCK1 and anti-ROCK2 were visualized using IRdye800-labeled goat-anti-rabbit IgG (H + L; Li-Cor). Blots were scanned with the Odyssey Imaging system (Li-Cor) and fluorograms were inverted for visualization. A down-regulation of beta-actin was observed during differentiation and fusion (Fig. 3A) as shown previously [36]. However, this was not a consequence of differences in protein loading as a Coomassie blue gel staining was similar in all experimental conditions (data not shown). Therefore beta-actin-corrected protein levels of RhoA, ROCK1, and ROCK2 were only compared within the same time-point (D0 or D3).

2.9. Immunocytochemistry of primary myotubes

For immunocytochemistry, cells were fixed using 4% (v/v) formaldehyde in PBS for 15 min and permeabilized in 0.5% (v/v) Triton X-100 in PBS for 20 min. After washing with 0.05% (v/v) Tween-20 in PBS, cells were blocked in blocking buffer containing 2% (w/v) bovine serum albumin (BSA), 2% (v/v) normal goat serum (NGS), 0.1% (v/v) Triton X-100, 0.05% (v/v) Tween-20, and 100 mM glycine in PBS for 30 min. To determine fusion, cells were incubated with mouse anti-Myosin (1:300, MF20 IgG2b; Developmental Studies Hybridoma Bank) in blocking buffer without glycine for 1 h. To determine tubulin morphology, cells were incubated with the primary antibody mouse anti-beta-tubulin (1:300, E7 IgG1; Developmental Studies Hybridoma Bank). Bound anti-beta-tubulin was visualized with AlexaFluor-488-labeled goat anti-mouse IgG1 (1:200; Molecular Probes) and anti-Myosin was visualized with AlexaFluor-594-labeled goat anti-mouse IgG2b (1:200; Molecular Probes). The cells were sealed using Vectashield mounting medium containing 4′,6-diamidino-2-phenylindole (DAPI), which stains all nuclei (Vector Laboratories, Burlingame, CA, USA) and visualized using the Zeiss Axiophot2 fluorescence microscope with Axiocam MRm CCD camera and photographed. Microscopy images were processed with the NIH ImageJ software using the background subtraction (rolling ball radius of 150 pixels) and automatically adjusted for brightness and contrast. The myoblast fusion index, which is the number of nuclei within the myotubes relative to the total number of nuclei was calculated using 5 different fields for each culturing condition ($N = 3$).

2.10. Cell viability assay

For cell viability, myoblasts/myotubes were stained with 20 μg/ml Hoechst 33342 (Life Technologies), 2 μM Yo-Pro-1-iodide (Life Technologies) and 1 μg/ml propidium iodide (PI; Sigma Aldrich) for 20 min at 37 °C to identify early apoptosis and necrosis, respectively [37]. The cells were visualized using the Zeiss Axiophot 2 fluorescence microscope with an Axiocam MRm CCD camera and photographed. From these images the number of nuclei in myoblasts/myotubes positive for Yo-Pro-1 and PI or Yo-Pro-1 alone relative to the total number of Hoechst 33342 positive nuclei was calculated using 5 different fields for each culturing condition ($N = 3$).

2.11. Statistical analyses

Average values are presented as mean ± SD. The myoblast fusion index of each culturing condition was tested for significance ($p < 0.05$) using either the one-way ANOVA or two-way ANOVA with a Bonferroni *post hoc* test. The results of the HEt oxidation were tested using a one-way ANOVA Kruskal–Wallis with a Dunns *post hoc* test. The results of the cell viability assay were tested using a two-way ANOVA with a Bonferroni *post hoc* test.

3. Results

Pilot studies revealed that myotube formation from primary myoblasts derived from murine skeletal muscle is inhibited in the presence of 100 nM ROT. This finding urged us to investigate whether this effect was general to CI inhibitors or specific to ROT. To address the specificity of the inhibitory effect of ROT, we decided to compare its effect with that of piericidin A (PA).

3.1. Lowest inhibitor concentration for maximal reduction of cellular oxygen consumption

CI inhibitors acutely decrease cellular oxygen consumption and for the purpose of standardization we first set out to establish the lowest inhibitor concentration that maximally reduced the rate of oxygen consumption. Both ROT and PA dose-dependently decreased the rate of oxygen consumption when added to a suspension of murine skeletal muscle-derived C2C12 myoblasts (Fig. 1A; half-maximal inhibitory concentrations of 10.06 ± 0.01 nM and 8.41 ± 0.01 nM, respectively). Both inhibitors virtually completely inhibited oxygen consumption and in both cases the lowest maximal inhibitory concentration was 100 nM. Myoblast fusion experiments last 3 days and Fig. 1B shows that oxygen consumption was still virtually completely inhibited in C2C12 myoblasts cultured for 3 days in proliferation medium containing 100 nM of either ROT or PA. These results indicate that both inhibitors remain effective during 3 days of chronic application.

3.2. Chronic rotenone exposure specifically and dose-dependently inhibits myoblast fusion

Primary myoblasts derived from murine skeletal muscle readily fused into large myotubes within 3 days after the onset of differentiation (Fig. 2A). Inclusion of 100 nM PA in the differentiation medium did not visibly affect myotube formation. In sharp contrast, however, the presence of 100 nM ROT clearly impaired this process in that fewer myotubes were formed, which, in addition, appeared smaller, thinner, and occasionally rounded. This visual impression was corroborated by calculation of the fusion index or the percentage of nuclei present in the myotubes. Fig. 2B shows that chronic ROT decreased this index dose-dependently, whereas chronic PA was without effect. The number of myogenin positive cells was not affected by ROT and PA (mean ± SD values of 79 ± 5%, 77 ± 3%, and 78 ± 4%, for vehicle (0.1% EtOH), ROT (100 nM), and PA (100 nM), respectively). ROT and PA also did not induce cell detachment as indicated by the absence of any significant change in the total number of nuclei (mean ± SD values of 100 ± 48%, 89 ± 47% and 80 ± 32%, for vehicle (0.1% EtOH), ROT (100 nM) and PA (100 nM), respectively). Additionally, myoblasts and myotubes were stained with Yo-Pro-1, PI, and Hoechst 33342 to determine cell death (Fig. 2C) after 3 days of differentiation. Only low numbers of nuclei in myoblasts/myotubes positive for Yo-Pro-1 and PI or Yo-Pro-1 alone were found, which did not significantly differ

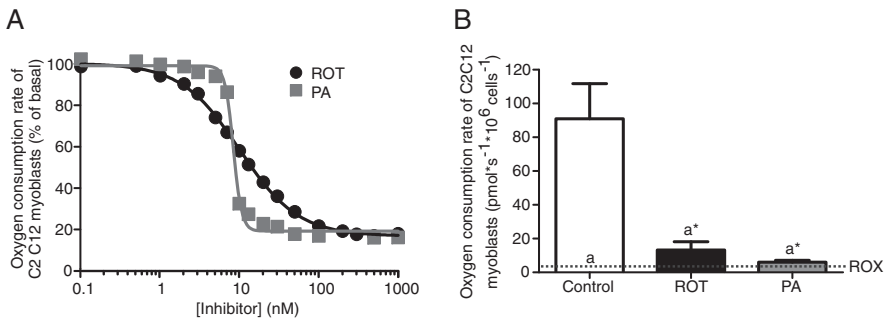

Fig. 1. Oxygen consumption of C2C12 myoblasts treated with rotenone and piericidin A. A) Oxygen consumption rates of C2C12 myoblasts in the presence of increasing concentrations (0–1000 nM) of rotenone (ROT) and piericidin A (PA). Oxygen consumption rates were normalized to basal respiration in the absence of inhibitor. B) Oxygen consumption rates of C2C12 myoblasts treated with 100 nM of ROT or PA for 3 days. The results ($N = 3$) are expressed as a mean ± SD and the dotted line represents the non-mitochondrial oxygen consumption rate (ROX). * significantly different from control ($p < 0.05$).

between control, ROT and PA. This indicates that cell death is not stimulated under these conditions.

Reactive oxygen species (ROS) are implicated in the differentiation and fusion of muscle cells [38] and ROT, when added at a concentration of 100 nM, readily stimulates the intracellular oxidation of HEt [39]. Both chronic ROT (100 nM) and PA (100 nM) showed a modest but significantly increased level of HEt-oxidizable ROS in myotubes after 3 days of differentiation (Fig. 2D). High concentrations of ROT are also known to disrupt the tubulin network, which could result in hampered myotube formation [25,40,41]. Such an off-target effect of ROT on the tubulin network should be most apparent in myoblasts as myotube formation is initiated by the fusion of functional myoblasts and requires remodeling of the myoblast tubulin network. To prevent this, the minimal concentration of ROT (100 nM) that maximally inhibited cellular oxygen consumption was used (Fig. 1A). At this concentration ROT did not visibly alter the tubulin network in primary myoblasts (Fig. 2E). This is in agreement with the observation that ROT did not induce microtubule disorganization in neurons [25]. As a positive control, nocodazole (500 nM, 24 h) [42] induced marked changes in tubulin network organization in myoblasts.

Taken together, the above results indicate that CI inhibition, cell death, and microtubule disorganization do not underlie the inhibitory effect of ROT on myotube formation and that, therefore, another mechanism should be considered. Below we explored this mechanism in more detail.

3.3. Rotenone-induced inhibition of primary myotube formation is primarily restored by ROCK2 knock-down

Evidence was provided that ROT affects the activities of several Rho-GTPases in neurons including RhoA [25]. RhoA and its effectors ROCK1/ROCK2 have been shown to be involved in myotube formation [28–33,43]. To address the possibility that ROT might exert its effect on myotube formation through these proteins, we performed specific knock-down experiments. Importantly, the transfection procedure did not increase Oas1 gene expression in primary myoblasts, indicating that the delivery of the siRNAs did not provoke an IFN response in these cells [44,45]. Twenty-four hours after the transfection and at the onset of differentiation (D0), the mRNA levels of RhoA, ROCK1, and ROCK2 in primary myoblasts were, relative to control (non-targeting siRNA), specifically and effectively knocked-down at the mRNA level by 97 ± 0.08%, 75 ± 30%, and 96 ± 3.3%, respectively. The knock-down remained very effective for 3 days during differentiation as the mRNA levels of RhoA, ROCK1, and ROCK2 in primary myotubes were still reduced by 88 ± 15.7%, 93 ± 5.0%, and 95 ± 0.8%, respectively. Western blot analysis of RhoA and ROCK1 confirmed the specificity and effectiveness of the knock-down approach at the protein level in myoblasts (D0) and myotubes (D3) (Fig. 3A). RhoA protein level was knocked-down by 95 ± 2.8% and 98 ± 2.8%, respectively, whereas ROCK1 protein level was completely knocked-down by 100% in myoblasts (D0) and myotubes (D3). However, ROCK2 expression was already very low in control (non-targeting) myoblasts (D0) and especially myotubes (D3), but a knock-down of 84 ± 12.6% in myoblasts (D0) and 69 ± 27.8% in myotubes (D3) to almost no detectable levels could still be observed. Nevertheless, this level of ROCK2 knock-down was able to fully prevent the ROT-induced inhibition of primary myotube formation whereas RhoA knock-down was ineffective (Fig. 3B and C). ROCK1 knock-down by itself tended to decrease the fusion index and, as a consequence, there was no significant inhibitory effect of ROT on myoblast fusion. However, when compared to the ROT-treated control, only knock-down of ROCK2, but not RhoA and ROCK1, significantly increased the fusion index to untreated control. We conclude that mainly ROCK2, independently from RhoA, is essential for ROT to exert its inhibitory effect on primary myotube formation.

3.4. Inhibition of Raf-1 activity prevents rotenone-induced inhibition of primary myotube formation

Activation of Raf-1 has been shown to inhibit muscle cell differentiation upstream of ROCK activity but also of MEK-ERK activity [30,46]. Therefore we pharmacologically inhibited Raf-1 activity by GW5074 and MEK-ERK activity by U0126 to investigate whether Raf-1, independently from MEK-ERK activity, is involved in the ROT-induced inhibition of myotube formation. As shown in Fig. 4, Raf-1 and MEK-ERK inhibition by GW5074 and U0126, respectively, did not affect the formation of myotubes at the highest concentration used (10 μM; Fig. 4A and B). However, in the presence of ROT (100 nM), only GW5074 but not U0126 restored myotube formation (Fig. 4A). Quantification of the fusion index (Fig. 4B) indicates that at 5 and 10 μM of GW5074 the ROT-induced inhibition of myotube formation was fully restored. In contrast, when similar concentrations of U0126 were used to inhibit MEK-ERK activity, myotube formation remained significantly decreased in the presence of ROT. This suggests that in the presence of ROT, Raf-1 activity, independently from MEK-ERK activity, is required to inhibit primary myotube formation.

4. Discussion

We demonstrate here for the first time that the ROT-induced inhibition of primary myotube formation requires active Raf-1 and ROCK2 and is independent of its inhibitory effect on CI-driven mitochondrial ATP production. We also show that inhibition of Raf-1 activity or ROCK2 knock-down alone does not significantly affect primary myotube formation. This altogether is favoring a model in which Raf-1 and ROCK2 most likely act, modulated by ROT, as negative regulators in the process of myotube formation. These conclusions are based on the following.

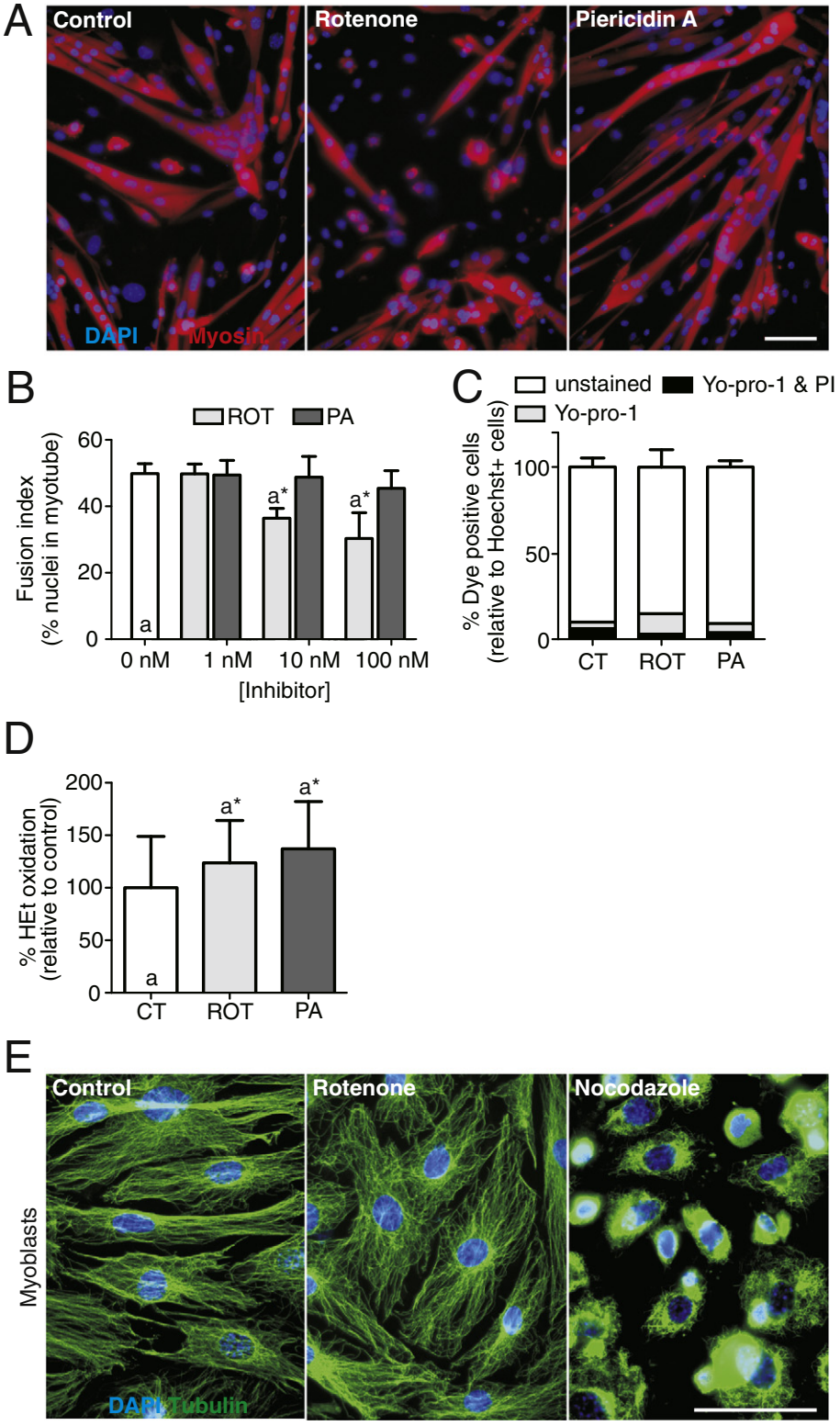

Fig. 2. Fluorescent immunocytochemistry and quantification of fusion index of primary myoblasts differentiated with rotenone and piericidin A. A) Primary myoblasts were differentiated in the presence of vehicle (control; left panel), 100 nM rotenone (middle panel) or 100 nM piericidin A (right panel) for 3 days, which resulted in a mixture of myoblasts and myotubes, which were fixed and then stained for DAPI (blue) and myosin (red). Scale bar represents 50 μm. B) Quantification of the myoblast fusion index, which is the number of nuclei within myotubes relative to the total number of nuclei, after a 3-day differentiation period of primary myoblasts in the presence of increasing concentrations (0–100 nM) of rotenone (ROT) or piericidin A (PA). The results ($N = 3$) are expressed as a mean ± SD. * Significantly different from control (0 nM; $p < 0.05$). C) Primary myoblasts were differentiated in the presence of vehicle (CT), 100 nM rotenone (ROT) or 100 nM piericidin A (PA) for 3 days, which were then stained with Yo-Pro-1, PI, and Hoechst 33342 to determine cell death. The results ($N = 3$) are expressed as a mean ± SD. D) Primary myoblasts were differentiated in the presence of vehicle (CT), 100 nM rotenone (ROT) or 100 nM piericidin A (PA) for 3 days, which resulted in a mixture of myoblasts and myotubes. Then fluorescence of HEt oxidation products was measured using live-cell microscopy in primary myotubes. The results (CT: $N = 134$; ROT: $N = 75$; PA: $N = 75$) are expressed as a mean ± SD. *Significantly different from control (CT; $p < 0.05$). E) Primary myoblasts were cultured in the presence of vehicle (control; left panel), 100 nM rotenone (middle panel) for 3 days or firstly for 2 days with vehicle and subsequently 1 day with 500 nM nocodazole (right panel). Myoblasts were then fixed and stained for DAPI (blue) and beta-tubulin (green). Scale bar represents 50 μm.

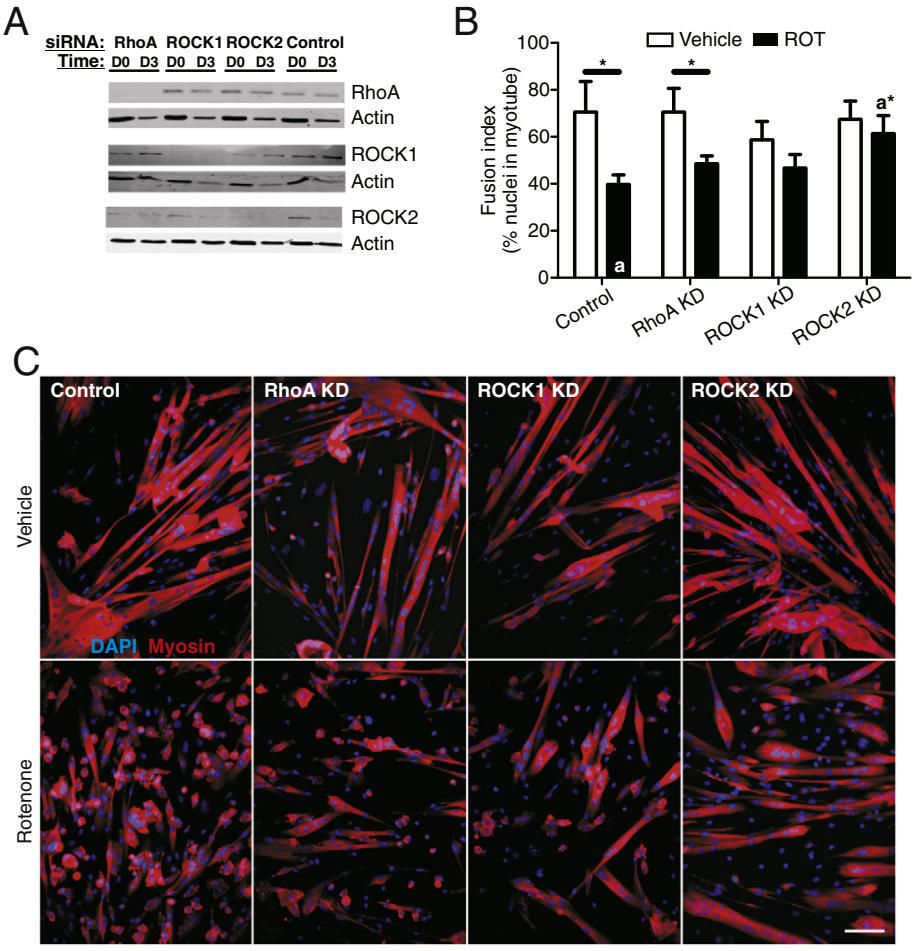

Fig. 3. Western blot, fluorescent immunocytochemistry and quantification of fusion index of primary myoblasts differentiated with rotenone after specific knock-down of RhoA, ROCK1 and ROCK2. A) Myoblasts were transfected with specific siRNAs: RhoA, ROCK1, ROCK2, and non-targeting (control) after which the protein expression levels of RhoA, ROCK1, ROCK2, and actin were analyzed in myoblasts (D0: 1 day after transfection) and myotubes (D3; 4 days after transfection and differentiation). B) The myoblast fusion index, which is the number of nuclei within myotubes relative to the total number of nuclei, is quantified of the different conditions described in panel C. The results ($N = 3$) are expressed as a mean ± SD. *Significantly different between the indicated conditions ($p < 0.05$). C) Control myoblasts (control; left panels) and myoblasts in which RhoA (middle left panels), ROCK1 (middle right panels), and ROCK2 (right panels) were specifically knocked-down (KD), were differentiated in the presence of vehicle (upper 4 panels) or 100 nM rotenone (lower 4 panels) for 3 days, which resulted in a mixture of myoblasts and myotubes, fixed and then stained for DAPI (blue) and myosin (red). Scale bar represents 50 μm.

It has been shown that active Raf-1 blocks myoblast differentiation either via regulating MEK-ERK activity [46] or ROCK activity [30]. However, in the latter study, inhibition of MEK-ERK activity was not sufficient to restore muscle cell differentiation, suggesting that primarily ROCK activity is involved. Moreover, differentiation and fusion of C2C12 myoblasts were inhibited when they expressed either a constitutively active RhoA or ROCK1 mutant [30–32,47]. In these studies, myoblast differentiation and fusion could be restored by pharmacological inhibition of ROCK by Y27632. However, Y27632 inhibits both ROCK1 and ROCK2 and might also display other side-effects. Therefore, we performed specific knock-down of RhoA, ROCK1, and ROCK2 in primary mouse myoblasts to decipher their individual roles in the ROT-induced inhibition of primary myotube formation. Here we demonstrate that this was primarily restored by knock-down of ROCK2, but not RhoA and to a lesser extent ROCK1. Based upon the mRNA levels, ROCK2 knock-down was very efficient, however, the magnitude of ROCK2 knock-down at the protein level appears to be less convincing. This is most likely due to the low ROCK2 signal found (with Western blot) in myoblast and especially in myotubes when transfected with non-targeting, RhoA and ROCK1 siRNA. Importantly, only in myoblasts in which ROCK2 was knocked-down, ROT was much less successful in preventing myotube formation. Especially because ROCK2 protein levels are not greatly reduced suggest that this protein is very important in mediating the ROT-induced inhibition of primary myotube formation.

The inhibitory effect of ROT on the formation of primary myotubes was also achieved by pharmacological inhibition of Raf-1 by GW5074 used at a concentration (5 μM) known to inhibit Raf-1 by at least 80%, but not of MEK-ERK by U0126. It has been demonstrated that GW5074 selectively acts on Raf-1 without significant effect on the activity of other proteins (i.e. cdk1, cdk2, cdk5, cdk6, c-src, p38 MAP kinase, VEGFR2, c-fms, JNK1-3, MEK1, MKK6, MKK7 and Gsk3β) [48,49]. Moreover, Raf-1 is ubiquitously expressed whereas A-Raf is expressed in several cell types (but not in skeletal muscle) and B-Raf is primarily expressed in the central nervous system [51,52]. This indicates that skeletal muscle (hence myoblasts/myotubes) primarily expresses Raf-1. It has been shown that GW5074 inhibits SIRT5 desuccinylation activity, however, this is minimally inhibited at 5 μM GW5074 [50], which exerts a maximum effect on myotube formation during chronic ROT treatment. Therefore it is unlikely that inhibition of SIRT5 desuccinylation activity plays any significant role in our studies. In the light of the above, we believe that our results with GW5074 support our conclusion that Raf-1 is involved in ROT-induced inhibition of myotube formation.

It was shown that ROT increased NADPH oxidase (NOX)-derived superoxide leading to neurotoxicity. This could be attributed to a direct

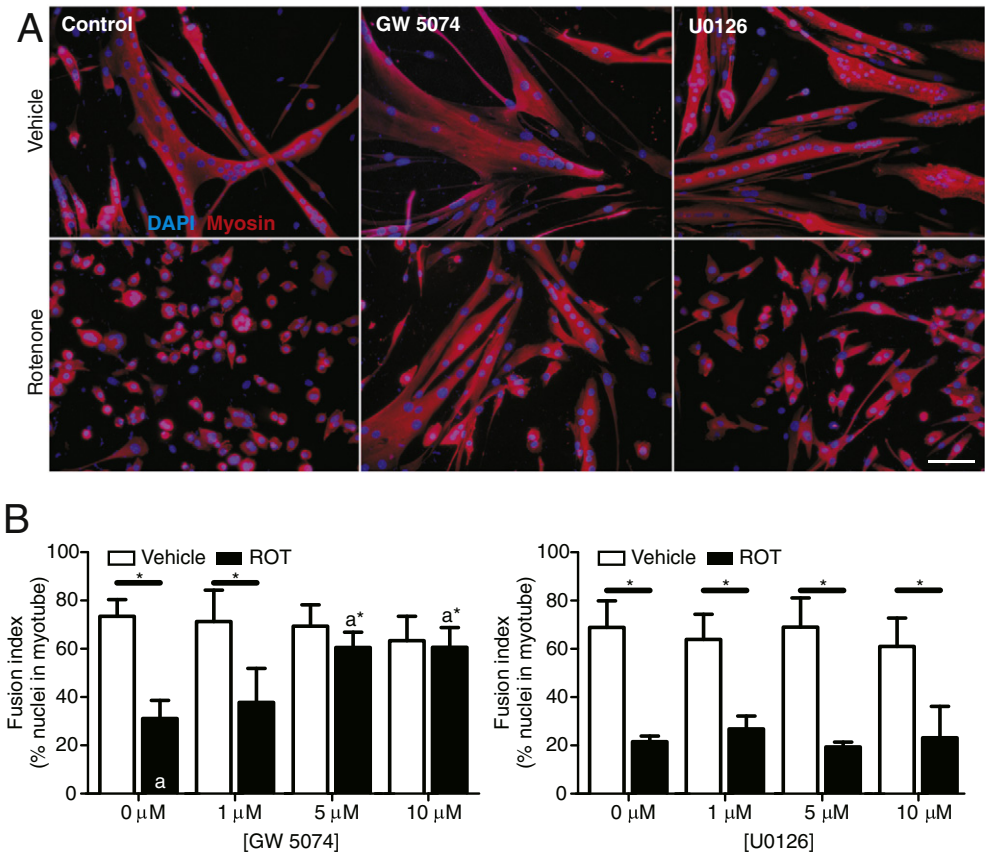

Fig. 4. Fluorescent immunocytochemistry and quantification of fusion index of primary myoblasts differentiated with rotenone and GW5074 or U0126. A) Vehicle- (left panels), GW5074- (middle panels), and U0126-treated (right panels) myoblasts were differentiated in the presence of vehicle (upper 3 panels) or 100 nM rotenone (lower 3 panels) for 3 days, which resulted in a mixture of myoblasts and myotubes, fixed and then stained for DAPI (blue) and myosin (red). Scale bar represents 50 μm. B) Quantification of the myoblast fusion index, which is the number of nuclei within myotubes relative to the total number of nuclei, after a 3-day differentiation period of primary myoblasts in the presence of increasing concentrations (0–10 μM) of GW5074 or U0126 and with or without 100 nM rotenone (ROT). The results ($N = 3$) are expressed as a mean ± SD. *Significantly different between the indicated conditions ($p < 0.05$).

interaction of ROT with gp91^{phox} and was found to be dependent on Rac1 activity [53–55]. Moreover, it was shown that ROT activates NOX in phagocytes and that upregulated NOX4 results in increased ROT-sensitive superoxide production in cardiac myocytes [54,56]. This indicates that ROT-induced activation of NOX is not specific to one cell type. In this sense, we observed that both ROT and PA stimulated oxidation of the ROS-sensor HEt to a similar extent (Fig. 2D), suggesting that HEt-oxidizing ROS derived from either CI inhibition or NOX activation is not responsible for the differential effect of ROT and PA on myotube formation. However, evidence in the literature suggests that both an increase and decrease in NOX4 expression can be associated with reduced myogenin mRNA levels in C2C12 cells. This is paralleled by a reduction in the number of myogenin positive C2C12 cells detected by immunocytochemical analysis [57]. This suggests that in the present study the ROT-induced inhibition of myotube formation could be a result of NOX4 activation. However, we did not observe such a reduction in myogenin positive myoblasts/myotubes and argues against a role for ROT-induced activation of NOX4 in ROT-induced inhibition of primary myotube formation.

In our experiments, individual and specific knock-down of RhoA, ROCK1, or ROCK2 in vehicle-treated cells did not significantly affect myotube formation. A similar lack of effect was observed in C2C12 myoblasts upon specific knock-down of ROCK2 and the ROCK2m isoform [58]. Similarly, knock-down of either ROCK1 or ROCK2 in C2C12 myoblasts only slightly increased myogenesis [30]. Strikingly, a recent study using stable knock-down clones of ROCK1 and ROCK2 in C2C12 myoblasts suggested that ROCK acted stimulatory on myotube formation [59]. However, the same study revealed that ROCK inhibition by Y27632 enhanced myotube formation. Similar to our knock-down experiments, we show that inhibition of Raf-1 activity alone does not significantly affect primary myotube formation. This suggests that Raf-1 and ROCK2 might not be essential for primary myotube formation, but are most likely negative regulators in this process.

We provide additional evidence indicating that the ROT-induced inhibition of primary myotube formation is most likely independent of its inhibitory effect on CI-driven mitochondrial ATP production. Firstly, this process was not hampered by the presence of the CI inhibitor PA (the binding pocket of which overlaps the CI binding pocket of ROT [60,61]) at a concentration at which this inhibitor virtually completely inhibited cellular oxygen consumption acutely and chronically (3 days). Secondly, a reduction in myotube formation was already observed at ROT concentrations (10 nM) that not fully blocked cellular oxygen consumption. Taken together, this suggests that ROT-induced inhibition of myotube formation is independent of CI-driven mitochondrial ATP production (i.e. fusion occurred normally in the presence of PA). We cannot entirely exclude CI to have a function in myotube formation as it might still play a different role apart from mitochondrial ATP production.

The finding above may also shed new light on results obtained in studies using ROT to demonstrate, among others, the role of CI and mitochondrial ROS levels in muscle differentiation [23]. In the latter study, ROT has shown to reduce the ROS levels and thereby inhibit myotube formation of H9c2 rat cardiac myoblasts. However, in our study, both chronic ROT and PA increased the levels of HEt-oxidizable ROS in murine primary myotubes. This favors the idea that differences

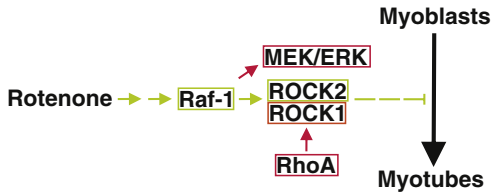

Fig. 5. Putative mechanism of how rotenone inhibits the formation of myotubes. Based on the results, the pathway in green (Raf-1/ROCK2) is suggested to be the mode of action, while the pathway in red (RhoA, MEK/ERK) is excluded and the pathway in orange (ROCK1) might contribute to a lesser extent. The mechanism of ROT interaction with Raf1 and/or ROCK2 and their down-stream targets remains unknown (dotted lines).

in inhibitor-induced ROS levels are not the mechanism of ROT-induced inhibition of primary myotube formation. Moreover, the lack of effect on myotube formation by chronic PA resembles more the finding that complex I deficiency induces myogenesis [62].

Next to this, the use of ROT as an agricultural pesticide and insecticide has been associated to the development of Parkinson's disease (PD) [63]. Rats and mice treated with ROT induced key features of PD [64,65] and some of these ROT-induced neurotoxic effects could be explained by the induction of neuronal apoptosis via Raf-1-MEK-ERK1/2 or inhibition of neuronal outgrowth via RhoA/ROCK [25,66]. However, in the latter study, Y27632 was used to inhibit ROCK signaling and thus our results may also provide more specific mechanistic insight in that Raf-1/ROCK2 pathway could be involved in the neurotoxic effects of ROT.

In summary, we conclude that ROT reduces the formation of myotubes in a manner that is independent of its inhibitory effect on CI-driven mitochondrial ATP production, but primarily requires the activity of the Raf-1/ROCK2 pathway, independently of RhoA and MEK-ERK (Fig. 5). However, it remains unknown (Fig. 5; two arrows) whether 1) ROT directly interacts with and increases the activity of Raf-1/ROCK2 or 2) exerts its effect via upstream activators of Raf-1 such as Ras, phosphatidylinositol 3-kinase, Cdc42/Rac, and/or Pak [67,68]. The effector mechanism of ROT-induced alteration of Raf-1/ROCK2 pathway on primary myotube formation also remains unknown (Fig. 5; dotted inhibitory line). For myotube formation to take place, a reorganization of the cytoskeleton in myoblasts is needed and F-actin depolarization is needed [69,70]. In contrast F-actin polymerization is stimulated by ROCK2 and might therefore be a potential effector mechanism [71–73]. However, many ROCK2-dependent substrates are involved in actin cytoskeleton rearrangements [71,73] and their identification will be of future investigation. Further, we show that Raf-1 and ROCK2 are not essential for myotube formation, but that upon activation (i.e. by ROT) this is inhibited, suggesting that this pathway is a negative regulator.

Most importantly, our results indicate that 1) ROT-induced inhibition of primary myotube formation requires Raf-1/ROCK2 activity, 2) ROT is not suited to study the effect CI-driven mitochondrial ATP production in primary murine myoblasts, 3) any effect of ROT should be carefully checked to specifically address its CI-independent side-effects, and 4) our results might provide new insight for the neurotoxic effects of ROT.

Authorships and disclosure

Conception and design of the study: SG, JW, RJ, PW, and WK. Performed the experiments and analyzed the data: SG, JW, and RJ. Wrote the paper: SG, PW, and WK. The authors declare that no competing interests exist.

Funding

This work was supported by an equipment grant from the Dutch Energy4All foundation and the CSBR (Centres for Systems Biology Research) initiative from the Nederlandse organisatie voor Wetenschappelijk Onderzoek (NWO, Netherlands Organisation for Scientific Research, Grant #CSBR09/013V). The funding organisations had no involvement in study design; collection, analysis and interpretation of data; writing of the report; and decision to submit the article for publication.

Acknowledgements

The Myosin (MF20) antibody developed by Donald A. Fischman and the beta-Tubulin antibody (E7) developed by Michael Klymkowsky were all obtained from the Developmental Studies Hybridoma Bank developed under the auspices of the NICHD and maintained by The University of Iowa, Department of Biological Sciences, Iowa City, IA 52242.

References

[1] W.J. Koopman, F. Distelmaier, J.A. Smeitink, P.H. Willems, OXPHOS mutations and neurodegeneration, EMBO J. 32 (2013) 9–29.
[2] W.J. Koopman, P.H. Willems, J.A. Smeitink, Monogenic mitochondrial disorders, N. Engl. J. Med. 366 (2012) 1132–1141.
[3] P. Mitchell, Coupling of phosphorylation to electron and hydrogen transfer by a chemi-osmotic type of mechanism, Nature 191 (1961) 144–148.
[4] W.J. Koopman, L.G. Nijtmans, C.E. Dieteren, P. Roestenberg, F. Valsecchi, J.A. Smeitink, P.H. Willems, Mammalian mitochondrial complex I: biogenesis, regulation, and reactive oxygen species generation, Antioxid. Redox Signal. 12 (2010) 1431–1470.
[5] A. Mauro, Satellite cell of skeletal muscle fibers, J. Biophys. Biochem. Cytol. 9 (1961) 493–495.
[6] A.R. Muir, A.H. Kanji, D. Allbrook, The structure of the satellite cells in skeletal muscle, J. Anat. 99 (1965) 435–444.
[7] C.K. Smith, M.J. Janney, R.E. Allen, Temporal expression of myogenic regulatory genes during activation, proliferation, and differentiation of rat skeletal-muscle satellite cells, J. Cell. Physiol. 159 (1994) 379–385.
[8] Z. Yablonka-Reuveni, A.J. Rivera, Temporal expression of regulatory and structural muscle proteins during myogenesis of satellite cells on isolated adult rat fibers, Dev. Biol. 164 (1994) 588–603.
[9] S. Grefte, S. Vullinghs, A.M. Kuijpers-Jagtman, R. Torensma, J.W. Von den Hoff, Matrigel, but not collagen I, maintains the differentiation capacity of muscle derived cells in vitro, Biomed. Mater. 7 (2012) 055004.
[10] P.S. Zammit, T.A. Partridge, Z. Yablonka-Reuveni, The skeletal muscle satellite cell: the stem cell that came in from the cold, J. Histochem. Cytochem. 54 (2006) 1177–1191.
[11] S. Grefte, A.M. Kuijpers-Jagtman, R. Torensma, J.W. Von den Hoff, Skeletal muscle development and regeneration, Stem Cells Dev. 16 (2007) 857–868.
[12] S.B. Charge, M.A. Rudnicki, Cellular and molecular regulation of muscle regeneration, Physiol. Rev. 84 (2004) 209–238.
[13] J.L. Vayssiere, L. Cordeau-Lossouarn, J.C. Larcher, M. Basseville, F. Gros, B. Croizat, Participation of the mitochondrial genome in the differentiation of neuroblastoma cells, In Vitro Cell. Dev. Biol. 28A (1992) 763–772.
[14] N.H. Herzberg, R. Zwart, R.A. Wolterman, J.P. Ruiter, R.J. Wanders, P.A. Bolhuis, C. van den Bogert, Differentiation and proliferation of respiration-deficient human myoblasts, Biochim. Biophys. Acta 1181 (1993) 63–67.
[15] W. Korohoda, Z. Pietrzkowski, K. Reiss, Chloramphenicol, an inhibitor of mitochondrial protein synthesis, inhibits myoblast fusion and myotube differentiation, Folia Histochem. Cytobiol. 31 (1993) 9–13.
[16] N. Hamai, M. Nakamura, A. Asano, Inhibition of mitochondrial protein synthesis impaired C2C12 myoblast differentiation, Cell Struct. Funct. 22 (1997) 421–431.
[17] P. Rochard, A. Rodier, F. Casas, I. Cassar-Malek, S. Marchal-Victorion, L. Daury, C. Wrutniak, G. Cabello, Mitochondrial activity is involved in the regulation of myoblast differentiation through myogenin expression and activity of myogenic factors, J. Biol. Chem. 275 (2000) 2733–2744.
[18] P. Seyer, S. Grandemange, M. Busson, A. Carazo, F. Gamaleri, L. Pessemesse, F. Casas, G. Cabello, C. Wrutniak-Cabello, Mitochondrial activity regulates myoblast differentiation by control of c-myc expression, J. Cell. Physiol. 207 (2006) 75–86.
[19] P. Seyer, S. Grandemange, P. Rochard, M. Busson, L. Pessemesse, F. Casas, G. Cabello, C. Wrutniak-Cabello, P43-dependent mitochondrial activity regulates myoblast differentiation and slow myosin isoform expression by control of Calcineurin expression, Exp. Cell Res. 317 (2011) 2059–2071.
[20] A.H. Remels, R.C. Langen, P. Schrauwen, G. Schaart, A.M. Schols, H.R. Gosker, Regulation of mitochondrial biogenesis during myogenesis, Mol. Cell. Endocrinol. 315 (2010) 113–120.
[21] D. Malinska, A.P. Kudin, M. Bejtka, W.S. Kunz, Changes in mitochondrial reactive oxygen species synthesis during differentiation of skeletal muscle cells, Mitochondrion 12 (2012) 144–148.
[22] P. Pawlikowska, B. Gajkowska, J.F. Hocquette, A. Orzechowski, Not only insulin stimulates mitochondriogenesis in muscle cells, but mitochondria are also essential for insulin-mediated myogenesis, Cell Prolif. 39 (2006) 127–145.

[23] S. Lee, E. Tak, J. Lee, M.A. Rashid, M.P. Murphy, J. Ha, S.S. Kim, Mitochondrial H_2O_2 generated from electron transport chain complex I stimulates muscle differentiation, Cell Res. 21 (2011) 817–834.
[24] W.S. Choi, R.D. Palmiter, Z. Xia, Loss of mitochondrial complex I activity potentiates dopamine neuron death induced by microtubule dysfunction in a Parkinson's disease model, J. Cell Biol. 192 (2011) 873–882.
[25] M. Sanchez, L. Gastaldi, M. Remedi, A. Caceres, C. Landa, Rotenone-induced toxicity is mediated by Rho-GTPases in hippocampal neurons, Toxicol. Sci. 104 (2008) 352–361.
[26] G. Carnac, M. Primig, M. Kitzmann, P. Chafey, D. Tuil, N. Lamb, A. Fernandez, RhoA GTPase and serum response factor control selectively the expression of MyoD without affecting Myf5 in mouse myoblasts, Mol. Biol. Cell 9 (1998) 1891–1902.
[27] R. Gallo, M. Serafini, L. Castellani, G. Falcone, S. Alema, Distinct effects of Rac1 on differentiation of primary avian myoblasts, Mol. Biol. Cell 10 (1999) 3137–3150.
[28] H. Heller, E. Gredinger, E. Bengal, Rac1 inhibits myogenic differentiation by preventing the complete withdrawal of myoblasts from the cell cycle, J. Biol. Chem. 276 (2001) 37307–37316.
[29] M. Meriane, P. Roux, M. Primig, P. Fort, C. Gauthier-Rouviere, Critical activities of Rac1 and Cdc42Hs in skeletal myogenesis: antagonistic effects of JNK and p38 pathways, Mol. Biol. Cell 11 (2000) 2513–2528.
[30] L. Castellani, E. Salvati, S. Alema, G. Falcone, Fine regulation of RhoA and Rock is required for skeletal muscle differentiation, J. Biol. Chem. 281 (2006) 15249–15257.
[31] S. Charrasse, F. Comunale, Y. Grumbach, F. Poulat, A. Blangy, C. Gauthier-Rouviere, RhoA GTPase regulates M-cadherin activity and myoblast fusion, Mol. Biol. Cell 17 (2006) 749–759.
[32] T. Nishiyama, I. Kii, A. Kudo, Inactivation of Rho/ROCK signaling is crucial for the nuclear accumulation of FKHR and myoblast fusion, J. Biol. Chem. 279 (2004) 47311–47319.
[33] E. Vasyutina, B. Martarelli, C. Brakebusch, H. Wende, C. Birchmeier, The small G-proteins Rac1 and Cdc42 are essential for myoblast fusion in the mouse, Proc. Natl. Acad. Sci. U. S. A. 106 (2009) 8935–8940.
[34] C.A. Collins, P.S. Zammit, Isolation and grafting of single muscle fibres, Methods Mol. Biol. 482 (2009) 319–330.
[35] E. Hutter, H. Unterluggauer, A. Garedew, P. Jansen-Durr, E. Gnaiger, High-resolution respirometry—a modern tool in aging research, Exp. Gerontol. 41 (2006) 103–109.
[36] L.J. Hayward, Y.Y. Zhu, R.J. Schwartz, Cellular localization of muscle and nonmuscle actin mRNAs in chicken primary myogenic cultures: the induction of alpha-skeletal actin mRNA is regulated independently of alpha-cardiac actin gene expression, J. Cell Biol. 106 (1988) 2077–2086.
[37] D. Gawlitta, C.W. Oomens, F.P. Baaijens, C.V. Bouten, Evaluation of a continuous quantification method of apoptosis and necrosis in tissue cultures, Cytotechnology 46 (2004) 139–150.
[38] E. Barbieri, P. Sestili, Reactive oxygen species in skeletal muscle signaling, J. Signal Transduct. 2012 (2012) 982794.
[39] W.J. Koopman, S. Verkaart, H.J. Visch, S. van Emst-de Vries, L.G. Nijtmans, J.A. Smeitink, P.H. Willems, Human NADH:ubiquinone oxidoreductase deficiency: radical changes in mitochondrial morphology? Am. J. Physiol. Cell Physiol. 293 (2007) C22–C29.
[40] B.R. Brinkley, S.S. Barham, S.C. Barranco, G.M. Fuller, Rotenone inhibition of spindle microtubule assembly in mammalian cells, Exp. Cell Res. 85 (1974) 41–46.
[41] L.E. Marshall, R.H. Himes, Rotenone inhibition of tubulin self-assembly, Biochim. Biophys. Acta 543 (1978) 590–594.
[42] A. Duckmanton, A. Kumar, Y.T. Chang, J.P. Brockes, A single-cell analysis of myogenic dedifferentiation induced by small molecules, Chem. Biol. 12 (2005) 1117–1126.
[43] M. Fortier, F. Comunale, J. Kucharczak, A. Blangy, S. Charrasse, C. Gauthier-Rouviere, RhoE controls myoblast alignment prior fusion through RhoA and ROCK, Cell Death Differ. 15 (2008) 1221–1231.
[44] A. Garcia-Sastre, C.A. Biron, Type 1 interferons and the virus–host relationship: a lesson in detente, Science 312 (2006) 879–882.
[45] C.A. Sledz, M. Holko, M.J. de Veer, R.H. Silverman, B.R. Williams, Activation of the interferon system by short-interfering RNAs, Nat. Cell Biol. 5 (2003) 834–839.
[46] B. Winter, H.H. Arnold, Activated raf kinase inhibits muscle cell differentiation through a MEF2-dependent mechanism, J. Cell Sci. 113 (Pt 23) (2000) 4211–4220.
[47] K. Iwasaki, K. Hayashi, T. Fujioka, K. Sobue, Rho/Rho-associated kinase signal regulates myogenic differentiation via myocardin-related transcription factor-A/Smad-dependent transcription of the Id3 gene, J. Biol. Chem. 283 (2008) 21230–21241.
[48] K. Lackey, M. Cory, R. Davis, S.V. Frye, P.A. Harris, R.N. Hunter, D.K. Jung, O.B. McDonald, R.W. McNutt, M.R. Peel, R.D. Rutkowske, J.M. Veal, E.R. Wood, The discovery of potent cRaf1 kinase inhibitors, Bioorg. Med. Chem. Lett. 10 (2000) 223–226.
[49] P.C. Chin, L. Liu, B.E. Morrison, A. Siddiq, R.R. Ratan, T. Bottiglieri, S.R. D'Mello, The c-Raf inhibitor GW5074 provides neuroprotection in vitro and in an animal model of neurodegeneration through a MEK-ERK and Akt-independent mechanism, J. Neurochem. 90 (2004) 595–608.
[50] B. Suenkel, F. Fischer, C. Steegborn, Inhibition of the human deacylase Sirtuin 5 by the indole GW5074, Bioorg. Med. Chem. Lett. 23 (2013) 143–146.
[51] L.B. Jilaveanu, C.R. Zito, S.A. Aziz, P.J. Conrad, J.C. Schmitz, M. Sznol, R.L. Camp, D.L. Rimm, H.M. Kluger, C-Raf is associated with disease progression and cell proliferation in a subset of melanomas, Clin. Cancer Res. 15 (2009) 5704–5713.
[52] J.C. Luckett, M.B. Huser, N. Giagtzoglou, J.E. Brown, C.A. Pritchard, Expression of the A-raf proto-oncogene in the normal adult and embryonic mouse, Cell Growth Differ. 11 (2000) 163–171.
[53] R. Pal, T.O. Monroe, M. Palmieri, M. Sardiello, G.G. Rodney, Rotenone induces neurotoxicity through Rac1-dependent activation of NADPH oxidase in SHSY-5Y cells, FEBS Lett. 588 (2014) 472–481.
[54] H. Zhou, F. Zhang, S.H. Chen, D. Zhang, B. Wilson, J.S. Hong, H.M. Gao, Rotenone activates phagocyte NADPH oxidase by binding to its membrane subunit gp91phox, Free Radic. Biol. Med. 52 (2012) 303–313.
[55] H.M. Gao, B. Liu, J.S. Hong, Critical role for microglial NADPH oxidase in rotenone-induced degeneration of dopaminergic neurons, J. Neurosci. 23 (2003) 6181–6187.
[56] T. Ago, J. Kuroda, J. Pain, C. Fu, H. Li, J. Sadoshima, Upregulation of Nox4 by hypertrophic stimuli promotes apoptosis and mitochondrial dysfunction in cardiac myocytes, Circ. Res. 106 (2010) 1253–1264.
[57] S. Acharya, A.M. Peters, A.S. Norton, G.K. Murdoch, R.A. Hill, Change in Nox4 expression is accompanied by changes in myogenic marker expression in differentiating C2C12 myoblasts, Pflugers Arch. - Eur. J. Physiol. 465 (2013) 1181–1196.
[58] M. Pelosi, F. Marampon, B.M. Zani, S. Prudente, E. Perlas, V. Caputo, L. Cianetti, V. Berno, S. Narumiya, S.W. Kang, A. Musaro, N. Rosenthal, ROCK2 and its alternatively spliced isoform ROCK2m positively control the maturation of the myogenic program, Mol. Cell. Biol. 27 (2007) 6163–6176.
[59] Y. Shibukawa, N. Yamazaki, E. Daimon, Y. Wada, Rock-dependent calponin 3 phosphorylation regulates myoblast fusion, Exp. Cell Res. 319 (2013) 633–648.
[60] D.J. Horgan, T.P. Singer, J.E. Casida, Studies on the respiratory chain-linked reduced nicotinamide adenine dinucleotide dehydrogenase. 13. Binding sites of rotenone, piericidin A, and amytal in the respiratory chain, J. Biol. Chem. 243 (1968) 834–843.
[61] G. Palmer, D.J. Horgan, H. Tisdale, T.P. Singer, H. Beinert, Studies on the respiratory chain-linked reduced nicotinamide adenine dinucleotide dehydrogenase. XIV. Location of the sites of inhibition of rotenone, barbiturates, and piericidin by means of electron paramagnetic resonance spectroscopy, J. Biol. Chem. 243 (1968) 844–847.
[62] J. Hong, B.W. Kim, H.J. Choo, J.J. Park, J.S. Yi, D.M. Yu, H. Lee, G.S. Yoon, J.S. Lee, Y.G. Ko, Mitochondrial complex I deficiency enhances skeletal myogenesis but impairs insulin signaling through SIRT1 inactivation, J. Biol. Chem. 289 (2014) 20012–20025.
[63] C.M. Tanner, F. Kamel, G.W. Ross, J.A. Hoppin, S.M. Goldman, M. Korell, C. Marras, G.S. Bhudhikanok, M. Kasten, A.R. Chade, K. Comyns, M.B. Richards, C. Meng, B. Priestley, H.H. Fernandez, F. Cambi, D.M. Umbach, A. Blair, D.P. Sandler, J.W. Langston, Rotenone, paraquat, and Parkinson's disease, Environ. Health Perspect. 119 (2011) 866–872.
[64] M. Inden, Y. Kitamura, H. Takeuchi, T. Yanagida, K. Takata, Y. Kobayashi, T. Taniguchi, K. Yoshimoto, M. Kaneko, Y. Okuma, T. Taira, H. Ariga, S. Shimohama, Neurodegeneration of mouse nigrostriatal dopaminergic system induced by repeated oral administration of rotenone is prevented by 4-phenylbutyrate, a chemical chaperone, J. Neurochem. 101 (2007) 1491–1504.
[65] F. Pan-Montojo, O. Anichtchik, Y. Dening, L. Knels, S. Pursche, R. Jung, S. Jackson, G. Gille, M.G. Spillantini, H. Reichmann, R.H. Funk, Progression of Parkinson's disease pathology is reproduced by intragastric administration of rotenone in mice, PLoS One 5 (2010) e8762.
[66] Y. Sai, J. Chen, Q. Wu, H. Liu, J. Zhao, Z. Dong, Phosphorylated-ERK 1/2 and neuronal degeneration induced by rotenone in the hippocampus neurons, Environ. Toxicol. Pharmacol. 27 (2009) 366–372.
[67] A.J. King, H. Sun, B. Diaz, D. Barnard, W. Miao, S. Bagrodia, M.S. Marshall, The protein kinase Pak3 positively regulates Raf-1 activity through phosphorylation of serine 338, Nature 396 (1998) 180–183.
[68] H. Sun, A.J. King, H.B. Diaz, M.S. Marshall, Regulation of the protein kinase Raf-1 by oncogenic Ras through phosphatidylinositol 3-kinase, Cdc42/Rac and Pak, Curr. Biol. 10 (2000) 281–284.
[69] M. Peckham, Engineering a multi-nucleated myotube, the role of the actin cytoskeleton, J. Microsc. 231 (2008) 486–493.
[70] N.T. Swailes, P.J. Knight, M. Peckham, Actin filament organization in aligned prefusion myoblasts, J. Anat. 205 (2004) 381–391.
[71] M. Amano, M. Nakayama, K. Kaibuchi, Rho-kinase/ROCK: a key regulator of the cytoskeleton and cell polarity, Cytoskeleton (Hoboken) 67 (2010) 545–554.
[72] J.C. Koch, L. Tonges, E. Barski, U. Michel, M. Bahr, P. Lingor, ROCK2 is a major regulator of axonal degeneration, neuronal death and axonal regeneration in the CNS, Cell Death Dis. 5 (2014) e1225.
[73] A.V. Schofield, O. Bernard, Rho-associated coiled-coil kinase (ROCK) signaling and disease, Crit. Rev. Biochem. Mol. Biol. 48 (2013) 301–316.